Permeability-Strength Relationships in Porous Materials

W. S. Rothwell* AND T. A. Dolton†

Lockheed Missiles and Space Company, Sunnyvale, Calif.

Design of systems utilizing porous materials, e.g., transpiration-cooled systems, may place requirements on both mechanical and flow-control (permeability) properties. Equations relating porosity and strength are developed assuming a simple cubic porous structure. The theoretical expressions are then compared with experimental data on porous beryllium and stainless steel materials, and good agreement is shown. Implicit relations are then developed which relate permeability to strength and density, and which include a material-dependent constant that is determined experimentally. Empirical fits to these relations are then manipulated to show some practical design consequences. It is seen that for a given material with required permeability for design, there is an optimum particle size which will yield maximum strength. The maximum strength, which varies with permeability to the minus $\frac{1}{4}$ power, is determined for the beryllium and stainless steel example materials. It is also seen that the relative density, for maximum strength, is 0.81 (porosity of 0.19) which is independent of the material and the permeability.

Nomenclature

A = flow cross-sectional area, cm^2
D = relative density, ρ/ρ_{max}
F = relative strength = σ/σ_{max}
k_0 = experimentally determined material constant, dimensionless
K = permeability, darcys (1 darcy = 9.87×10^{-9} cm^2 = 1.062×10^{-11} ft^2)
L = unit cell size, cm
L_e = effective flow path length, Eq. (8)
p = pressure, ksi
P = porosity = $(1 - D)$
r = contact radius, cm
R = ratio of change in permeability to change in density
s = flow length, cm
S = specific internal surface area, cm^{-1}
t = time, sec
v = fluid velocity, cm/sec
V = volume, cm^3
X = dimensionless compaction variable = r/L
y = coordinate in flow direction, cm
ρ = density, gm/cm^3
σ = strength, ksi

Subscripts

c = constriction
f = fluid
m = optimum value to yield maximum strength
max = maximum value for given particle size
o = uncompacted state
solid = solid fraction of total volume

Introduction

INTEREST in permeable porous media stems from their applications in transpiration cooling, flow contour control, and filtering. Early applications of permeable porous media were primarily for filters and absorbers where strength and accurate permeability control were not critical. In more recent uses, such as transpiration cooling, when heating rates are extreme, large coolant flow rates must pass through the material to permit adequate cooling; as a result, large pressure differentials may exist across the thickness of the material. Extreme pressure gradients may also be present on one side of the porous media (e.g., along the exterior of a re-entry vehicle), further complicating the stress field. In this application structural as well as thermodynamic performance is critical.

To determine the properties required of a porous material in an application such as transpiration cooling, it is necessary to conduct a preliminary design analysis. The design analysis begins with establishing the thermodynamic performance: pressure and temperature of coolant and matrix necessary to meet given performance criteria (e.g., prevent the material from melting). The key material property requirement, which may be determined in this step, is the permeability. The questions then arise: For this given permeability, what is the optimum porosity to permit maximum strength of the material? What is the maximum strength which can be attained? What particle size should be used to achieve maximum strength? To answer these questions for preliminary design studies, it is useful to consider the analytical relationships among permeability, porosity, particle size, pore size, and strength.

These relationships can aid the materials engineer in establishing porosity goals and, in the case of powder metallurgy, the goals for particle size, which will yield a workable design. The purpose of this paper is to develop these relationships for simple spherical particle arrays and establish some conclusions which affect production of porous materials.

Typical powder particles used in sintering and hot-pressing have rough surfaces and a variety of shapes. Nevertheless, it will be shown that this theoretical analysis is equally useful for relating the properties of a commercial powder and of a special powder of spherical particles.

Much attention has been given in the literature to the relation between permeability and porosity and reviews are available by Scheidegger[1] and Collins.[2] Also, the variation of strength with porosity has been considered frequently.[3-8] However, we found that further work was necessary to develop expressions relating permeability and strength and in the interpretation of these and other relationships for application in producing porous material with specified permeability, strength, and particle size.

Experimental Data

Two sources of experimental data will be used to compare with theoretical derivations. One is the result of work performed at the Lockheed Missiles and Space Company on the
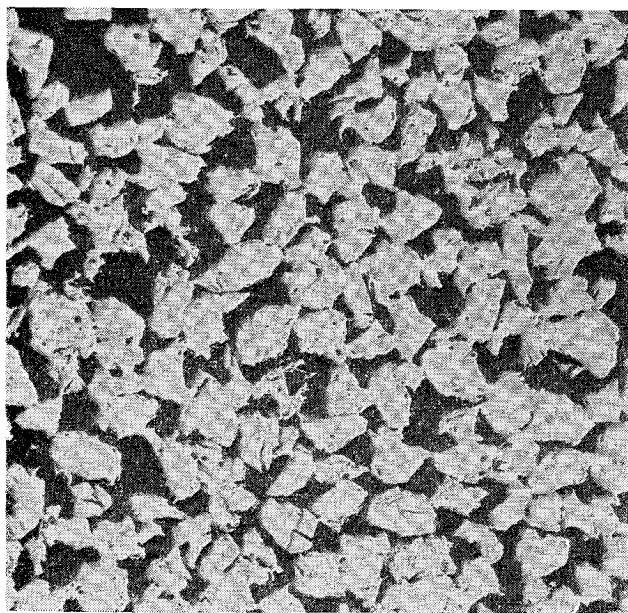
Fig. 1   Photomicrograph of 80% dense sintered porous beryllium, mag. 50×.

Fig. 2   Model of compressed simple cubic array of spheres used in theoretical calculations.

development of porous beryllium materials for transpiration cooling applications. Property data from this source is listed in Table 1. The starting material used was as-received or screened fractions of Berylco grade SS beryllium powder. The powder fractions consisted of fairly uniform size particles with rough surfaces and irregular shapes. This powder was then sintered by a special technique to the desired density. Figure 1 is a photomicrograph of a sintered Be body with density of 80%. Permeability values were determined by using Darcy's Law

$$v = -K\rho_f dp/dy$$

and measurements of water flow rate under a pressure differential of one atmosphere. These were divided by the square of the mean particle diameter to obtain a dimensionless relative number. The relative strengths were determined from tensile test values divided by the strength of 100% dense beryllium with a grain size equal to the particle size used.[9] This was, for example, 43 ksi for 50 μ particles. The second source of data is a report by Heck, Ferriss, Mott, and Comstock on porous materials prepared from type 301
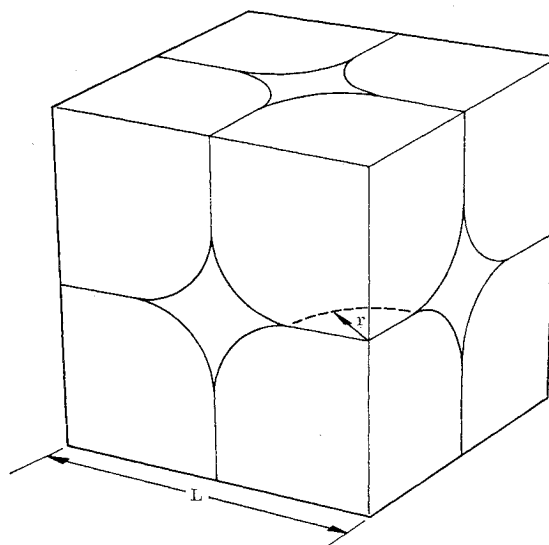
and 302 stainless steel spherical powders.[10] Their permeability measurements were made with air as the fluid. Allowance for the resultant deviation from Darcy's equation was made by using the slope of the flow rate vs pressure differential curve near the origin to compute permeability. We use their data on four different spherical powder sizes for each steel type. For the type 302, the mean particle diameters are 160, 215, 275, and 360 μ. For the type 301 the diameters are 52, 68, 89, and 126 μ. Relative strengths were obtained from their tensile strengths by dividing by a 100% dense value. This value was obtained by plotting the tensile strengths versus density for each particle size and extrapolating to the 100 percent value. The average of these was about 130 ksi for the type 301 and 60 ksi for the type 302.

Theoretical Analysis

Relation between Density and Strength

Various expressions have been derived to relate density and strength for porous materials based on different theoretical models.[3-8] The most simple approach is to assume a simple cubic array of spheres which are compressed to form

Table 1   Properties of sintered porous beryllium

Relative density	Particle size range (μ)	Mean particle diam (μ)	Tensile strength (ksi)	σ/σ_{max}	Permeability (Darcys)	$10^{-2}K/L_o^2$ (Darcys/cm^2)
0.700	<44	30	8.30	0.15	0.0212	23.5
0.725	<105	40	8.55	0.18	0.0149	9.32
0.765	<105	40	14.05	0.30	0.0077	4.81
0.770	44–61	50	12.40	0.29	0.0150	6.00
0.780	61–74	65	9.55	0.26	0.0265	6.27
0.790	61–74	65	12.30	0.33	0.0420	9.94
0.794	61–74	65	10.00	0.27	0.0600	14.2
0.796	<105	40	12.60	0.27	0.0055	3.43
0.798	44–61	50	13.70	0.32	0.0163	6.52
0.805	61–74	65	14.00	0.37	0.0160	3.79
0.805	61–74	65	15.50	0.42	0.0130	3.08
0.805	61–74	65	11.50	0.31	0.0140	3.31
0.815	<105	40	19.45	0.41	0.0035	2.19
0.816	<105	40	17.70	0.37	0.0079	4.93
0.820	<44	30	19.60	0.36	0.0018	2.00
0.833	44–61	50	18.10	0.43	0.0042	1.68
0.835	30–44	35	20.10	0.40	0.0030	2.45
0.842	61–74	65	20.85	0.56	0.0049	1.16
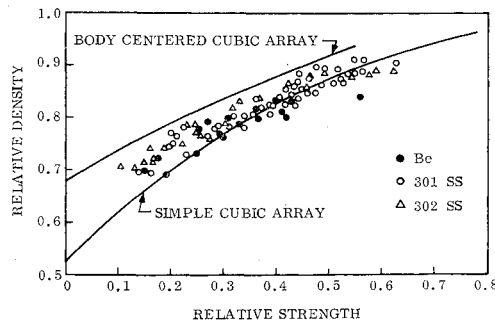
Fig. 3 Plots of relative strength vs relative density for two theoretical models and experimental data points for porous beryllium and porous stainless steel.

circular areas of contact as shown in Fig. 2. Using this model, Knudsen[6] has shown that the relationship can be approximated by an exponential form,

$$\sigma = \sigma_{max} e^{-aP} \qquad (1)$$

where P is porosity and σ is strength. σ_{max} represents the maximum strength obtainable in the solid (nonporous) material for a given initial particle size, L_o.

The assumption is made that the ultimate strength is determined by failure at the area of contact between spheres. Using this criterion and the geometric relationships for the model, the solution for strength and density can be expressed parametrically as,

$$F \equiv \sigma/\sigma_{max} = \pi X^2 \qquad (2)$$

$$D = (\pi/6)[3(1 + 6X^2) - 2(1 + 4X^2)^{3/2}] \qquad (3)$$

where D is relative density, and $X = r/L$, where r is the radius of the circular area of contact between spheres, and L is the unit cell size; Eqs. (2) and (3) hold only for $0 \leqslant X \leqslant 0.5$. The expressions for $0.5 \leqslant X \leqslant 0.707$ have been obtained, also, but are very lengthy and of no interest for
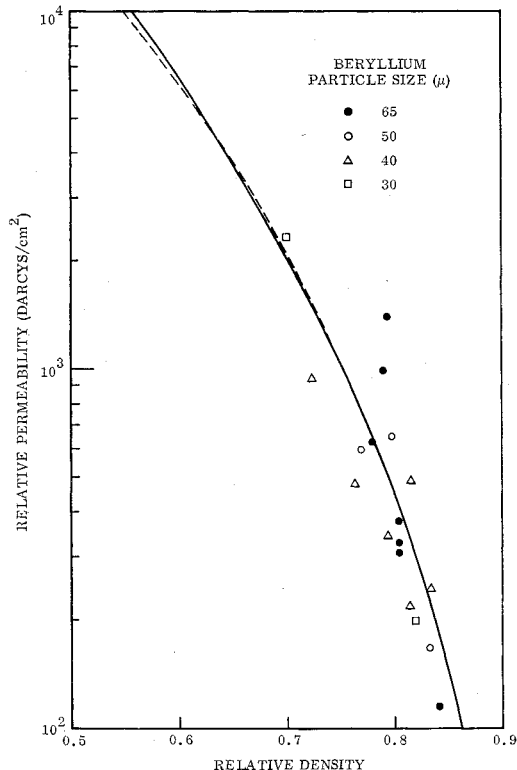
Fig. 4 Theoretical plot of relative permeability vs relative density and experimental data points for porous beryllium. Dashed line shows fit of empirical expression.

permeability analysis because they represent the region of closed porosity.

An analysis has been made, also, of the body-centered cubic model of packed spheres. The relations for this model are

$$F = (8)^{1/2}\pi X^2 \qquad (4)$$

$$D = 4\pi[(3)^{1/2}(X^2 + 0.125) - 2(X^2 + 0.188)^{3/2}] \qquad (5)$$

$$0 \leqslant X \leqslant 0.25$$

The theoretical relations between relative density and relative strength are shown in Fig. 3 for the two models along with the experimental values. The real situation appears to lie somewhere between the two models. However, a reasonably good fit is observed for the simple cubic model. Therefore, this model was used in extension of the analysis to permeability relationships.

Permeability Relations

Theoretical expressions relating permeability to relative density, D, and relative strength, F can be obtained using the results derived above and an equation of the Kozeny-Carman type (Ref. 1, see p. 129) relating specific internal surface area, S (ratio of internal surface area to total volume), and permeability, K. Strictly speaking, flow equations based on hydraulic radius theory, such as the Kozeny-Carman equation, are only valid for unconsolidated media with random pore structure. However, reasonably good agreement has been obtained for consolidated media with equations employing a tortuosity factor equal to the ratio of the effective path length to the true thickness, L_e/L.[11] Accordingly, we have adopted the following flow equation form (Ref. 11, p. 13),

$$K = (L/L_e)^2(1 - D)^3/k_o S^2 \qquad (6)$$

where k_o is an empirical constant determined by experiment for each material.

To relate this equation to the simple cubic packed sphere model, the ratio of the effective to the direct path length can be approximated as the ratio of the time for flow to take place through the actual geometry of a unit cell to that for direct flow through a pipe with the area, A_c, of the smallest constriction, i.e., $L_e/L = t/t_c$. Assume constant flow rate, velocity through the constriction, v_c, velocity and area at any cross section, v and A. Then, for an incompressible fluid $v = v_c A_c/A$,

$$t_c = L/v_c, \text{ and } t = \int ds/v.$$

Therefore,

$$L_e/L = t/t_c = (1/A_c L)\int A ds$$

Since,

$$\int A ds = \text{void volume} = (1 - D)L^3,$$

$$L/L_e = A_c/L^2(1 - D) \qquad (7)$$

Note that this is also equivalent to setting the effective path length equal to the void volume divided by the area of the constriction. From the geometry,

$$A_c/L^2 = 1 - 2X -$$
$$(1 + 4X^2) \arctan[(1 - 2X)/(1 + 2X)] \qquad (8)$$

and

$$SL = \pi(1 + 4X^2)[1.5(0.25 + X^2)^{-1/2} - 2] \qquad (9)$$

We will need to know, also, the relation between actual and original particle size, i.e., L/L_o. The ratio L/L_o is obtained from the fact that $DL^3 = V_{solid}$ and the assumption that the solid volume is a constant independent of processing

variables and distortion of orginal particle shape. This ratio is then

$$L/L_o = (\pi/6D)^{1/3} \tag{10}$$

Now, expressing permeability in a dimensionless form relative to particle size, i.e., as K/L_o^2, we can write Eq. 6 in the following form and with a factor to give units of darcys/cm²:

$$K/L_o^2 = (6.55 \times 10^7/k_o)(A_c/L^2)^2 \times$$
$$(1 - D)(L/L_o)^2/(SL)^2 \tag{11}$$

By varying X and using Eqs. (2, 3, 8, 9, 10, and 11) we can establish the implicit relations for a given material, i.e., a given k_o:

$$K/L_o^2 = f_1(D) \tag{12}$$

and

$$K/L_o^2 = f_2(F) \tag{13}$$

This has been done using a simple computer program. Figures 4, 5, and 6 show the permeability-density relation, Eq. (12), and compare the theory to data for Be, type 301 SS and type 302 SS, respectively. For the beryllium it was necessary to choose a k_o equal to 15.6 while for both stainless steels k_o was taken as 1.0. The factor of 15.6 between the k_o for beryllium and that for stainless steel could be explained on the basis of the increased surface area per unit volume of the Be particles compared to the spheres assumed in the derivation. From Fig. 1 it can be seen that the Be particle shape can be approximated by prolate ellipsoids with an axial ratio of 2:1. Such particles have a surface to volume ratio about twice that of spheres. The surface of the par-

ticles is obviously rough also (the spherical steel particles were quite smooth) so an additional factor of 2 would not be unreasonable. The total increased surface area effect would then be 4^2 or 16 which would account by itself for the observed factor of 15.6. Differences in wettability, friction coefficients, and other factors undoubtedly must also have some influence. In any case, it is apparent that the shape of the theoretical curve fits the experimental data very well. This supports the validity of the assumptions made in the derivation. The value of explaining differences in vertical displacement of the curves comes from the insight it provides for predicting behavior of other materials. The reliability of such predictions will increase as k_o is determined for more materials.

Using the values of k_o determined from the fit of the K/L_o^2 versus D [Eq. (12)] curves, the K/L_o^2 vs F [Eq. (13)] curves can be plotted and compared with the experimental data. This is done in Figs. 7, 8, and 9 for the Be, type 301 and 302 stainless steels, respectively. It can be seen that the data fit the shape of the curve in all cases, but fall below them in the case of the stainless steels. We interpret this as an indication that the greater difficulty of sintering spherical powders (steel) compared to rougher aspherical powders with large surface energy (beryllium) has resulted in relatively weaker porous materials for the steels. Stated another way, the effective bonding strength, based on the assumed contact area to volume ratio, is less for the spherical steel powders than for the Be powder.

In order to make further useful analysis, empirical expressions have been determined which closely fit the exact theoretical curves over the range of interest. These are,
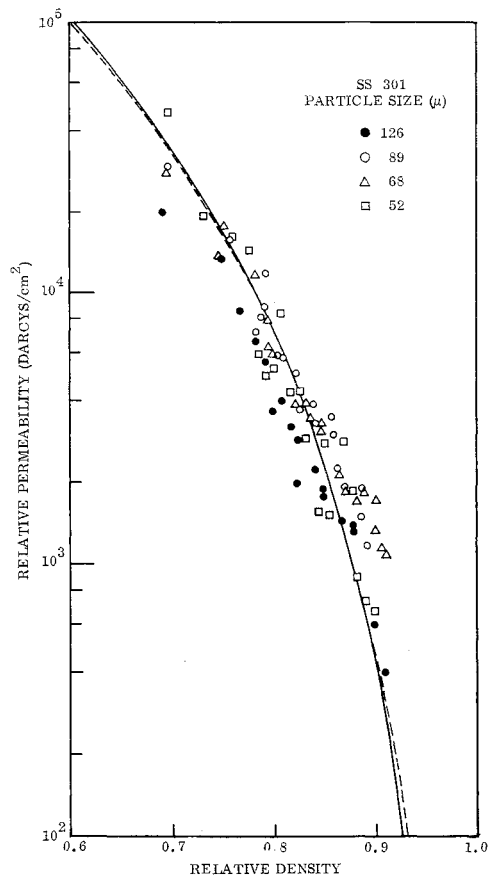
$$K/L_o^2 = c(1 - D)^3(1 - D^2) \tag{14}$$

Fig. 5   Theoretical plot of relative permeability vs relative density and experimental data points for porous type 301 stainless steel. Dashed line shows fit of empirical expression.
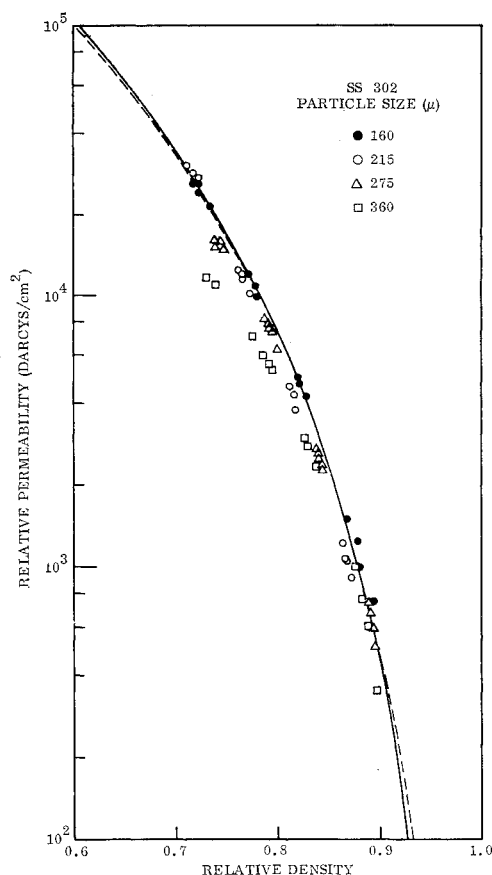
Fig. 6   Theoretical plot of relative permeability vs relative density and experimental data points for porous type 302 stainless steel. Dashed lines shows fit of empirical expression.
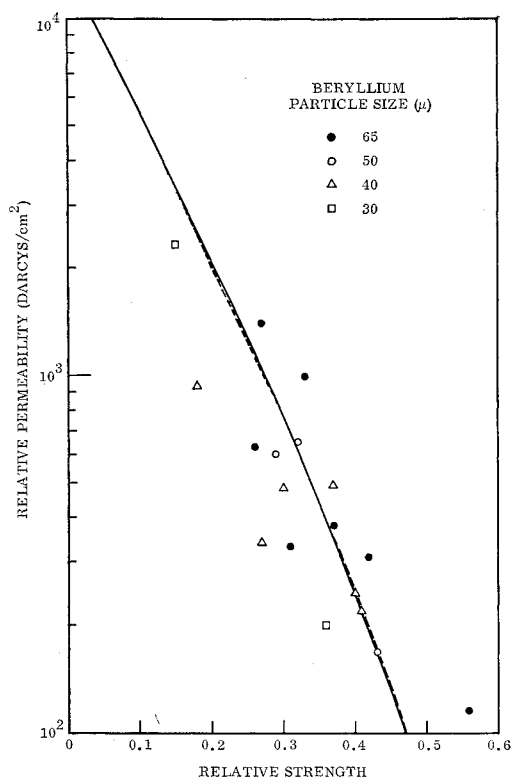
Fig. 7   Theoretical plot of relative permeability vs relative strength and experimental data points for porous beryllium.   Dashed line shows fit of empirical expression.

where

$$c = 2.42 \times 10^6/k_o$$

thus

$$c = 1.55 \times 10^5 \text{ for beryllium}$$

$$c = 2.42 \times 10^6 \text{ for stainless steel}$$
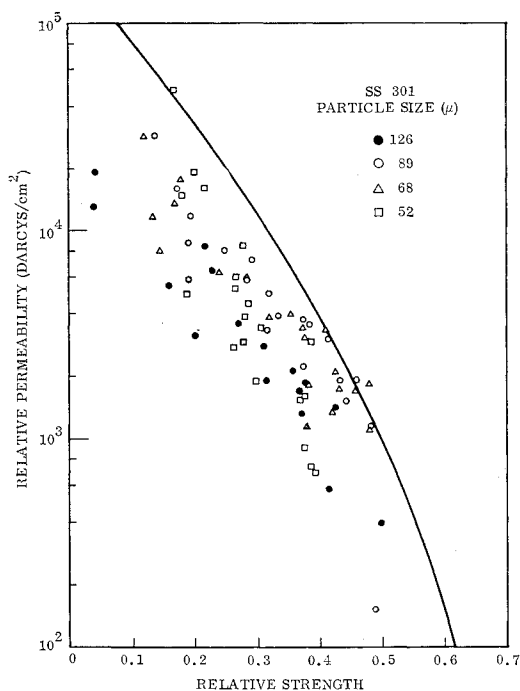

Fig. 8   Theoretical plot of relative permeability vs relative strength and experimental data points for porous type 301 stainless steel.   Empirical curve coincides with theoretical plot.
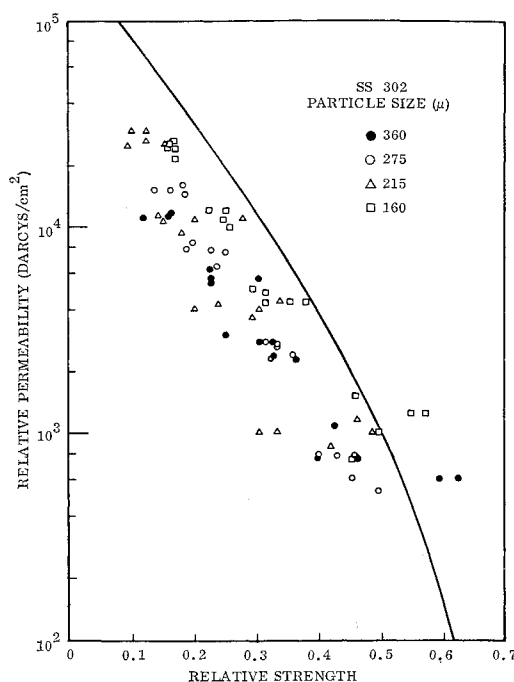

Fig. 9   Theoretical plot of relative permeability vs relative strength and experimental data points for porous type 302 stainless steel.   Empirical curve coincides with theoretical plot.

and

$$K/L_o^2 = d \exp[-9.57F(1 + 2F^4)] \qquad (15)$$

where

$$d = 2.17 \times 10^5/k_o$$

thus

$$d = 1.39 \times 10^4 \text{ for beryllium}$$

$$d = 2.17 \times 10^5 \text{ for stainless steel}$$

The small deviations of these expressions from an exact fit are shown by the dotted lines in Figs. 4–9.

Analysis of Permeability-Density-Strength Relations

The relationships derived above among permeability, density and strength may now be used to determine characteristics of porous materials which are important in design, and to determine limitations in material strengths when controlled permeability is desired.   These results are discussed in the following paragraphs.

Consider first the variation of permeability with the density. The ratio of the relative change in permeability to the relative change in density is $(D/K) \, dK/dD = R$.   Taking the derivation of Eq. (14) and making the proper substitutions yields

$$R = -(5D + 3)D/(1 - D^2) \qquad (16)$$

A plot of R for values of relative density, D, between 0.5 and 1 is shown in Fig. 10.   It is apparent that permeability is very sensitive to variations in density, especially for the most dense material.   This makes very clear the necessity for precise control of density in order to obtain accurate, uniform and reproducible values of permeability.

By examining Eq. (15) in terms of the variation of F with L_o, it would seem that maximum strength is available for maximum particle size, L_o.   However, insofar as grain size can be related to particle size, σ_{max} is actually a function of L_o through the Griffith-Orowan relation[6] which can be
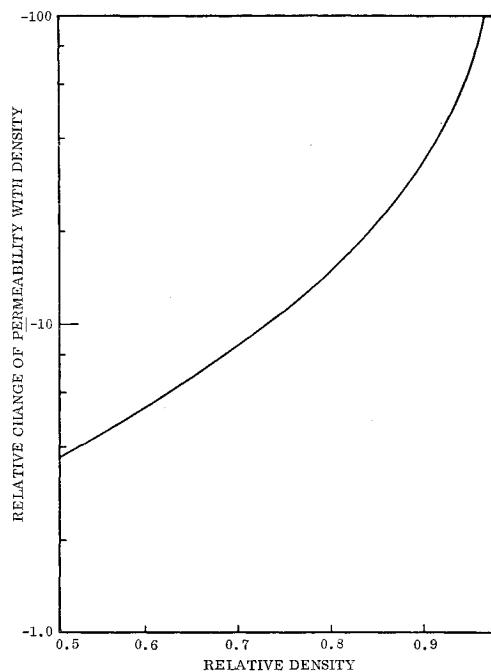
Fig. 10 Theoretical plot showing how the amount of change of permeability with a change in density depends upon density.

written,

$$\sigma_{max} = gL_o^{-1/2} \tag{17}$$

Thus, a correct examination of the variation of σ with L_o shows that for any given K it has a maximum for some optimum value of L_o, which we label L_m.

For L_o greater than L_m the grain size is too large for good strength. For L_o less than L_m the particles must be less tightly packed in order to give the required permeability, and thus give lower strength. The relation between L_m and K is found by substituting the definition of F ($F \equiv \sigma/\sigma_{max}$) and Eq. (17) into Eq. (15), taking the derivative of σ with respect to L_o in Eq. (15) and setting $d\sigma/dL_o$ equal to zero. This leads to the determination of an optimum $F_m = 0.357$, a constant, independent of g, d, and L_o. Thus, for a given K the choice of an $L_o \equiv L_m$ to give maximum strength, σ, will always result in the same optimum relative strength, F_m. The optimum particle size, L_m, for maximum strength at a given K is found by substituting F_m into Eq. (15) and solving for L_m.

Thus

$$L_m = hK^{1/2} \tag{18}$$

where

$$h = 1.26 \times 10^{-2}k_o^{1/2}$$

and

$$h = 4.98 \times 10^{-2} \text{ for Be}$$

$$h = 1.26 \times 10^{-2} \text{ for SS}$$

A plot of L_m versus K is shown in Fig. 11 for both materials along with data for the porous materials with densities within 1% of the optimum density (see below). A further significant finding is made by solving for $D = D_m$ by substituting the value of L_m from Eq. (18) into Eq. (14) (or by entering the appropriate graph with $1/h^2 = K/L_m^2$). This finding is that there is an optimum density, $D_m = 0.808$, which, like F_m, is independent of the particle size and material. Finally, we can obtain an expression for the maximum obtainable tensile strength, which will vary with par-
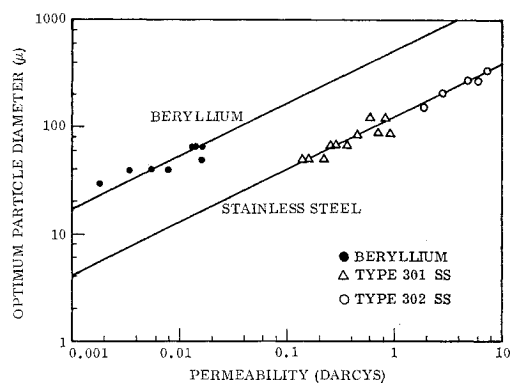

Fig. 11 Theoretical plots of optimum particle size for maximum strength vs permeability for porous beryllium and porous stainless steel. Experimental data points are shown for porous beryllium and porous stainless steels of optimum density.

ticle size, or, as seen from Eq. (18), with permeability. This is done by combining the definition for F, Eqs. (17) and (18) (with appropriate constants obtained experimentally), and the above value for F_m. The resultant expression for maximum obtainable strength in ksi is,

$$\sigma_m = jK^{-1/4} \tag{19}$$

where

$j = 4.71$ for beryllium

$j = 38.0$ for 301 stainless steel

$j = 32.0$ for 302 stainless steel

This relation is plotted for the three materials in Fig. 12 along with data for the porous materials with densities within one percent of the optimum density. It can be seen that the porous beryllium strengths were near the maximum while those for the stainless steel fell below, possibly because of the difference in sinterability discussed previously.

Concluding Remarks

The preceding analysis has shown that permeability, density, and strength of porous materials are interrelated in a nontrivial manner, and thus analytical procedures such as this may be applied to guide the development of porous materials in optimizing these variables for a given system. Although the derivations were based on an idealized system of particle shape and arrangement their application to the
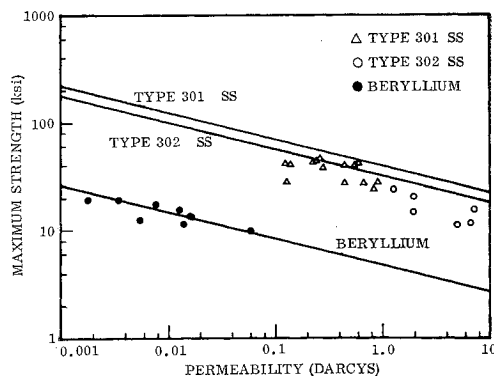

Fig. 12 Theoretical plots of maximum strength obtainable vs permeability for porous beryllium and stainless steel with optimum density and particle size. Experimental data points are shown for porous beryllium and porous stainless steels of optimum density.

relations between properties of real porous materials was clearly demonstrated.

To recap the technique used to arrive at the relationships just developed.

1) A geometric relationship was derived between strength and density assuming a simple arrangement of spherical particles [Eqs. (2) and (3)], and good agreement was shown with experimental data.

2) Employing the Kozeny-Carman relation [Eq. (6)] and geometric expressions relating surface area, constriction area, tortuosity factor and particle size [Eqs. (7–10)], an implicit relation was obtained between permeability, initial particle size and density [Eq. (12)], and another for strength [Eq. (13)].

3) These implicit relations were seen to fit the shape of experimental data; an experimentally-determined constant was employed which yielded good numerical agreement.

4) It was shown that there is an optimum particle size which will produce maximum strength of the material, for a given permeability. Also, it was shown that, by control of particle size, the relative density of the system is a constant for maximum strength. It is noted that these results are general within the above model and are not dependent on the particular form of the empirical relations used [Eqs. (14) and (15)].

In applying a material to a given set of design requirements, one must decide on priorities between strength and permeability values and accept a system which, in general, is not optimum for both. The procedure developed here can be utilized to provide the necessary quantitative analysis for this decision. Such a procedure will also indicate the particle sizes needed to achieve the desired properties. It is then the job of the material fabricator to produce the required material.

References

[1] Scheidegger, A. E., *Physics of Flow through Porous Media,* Macmillan, New York, 1960, p. 129.

[2] Collins, R. E., *Flow of Fluids through Porous Materials,* Reinhold, New York, 1961.

[3] Bal'shin, M. Y., "Relation of Mechanical Properties of Powder Metals and their Porosity and the Ultimate Properties of Porous Metal-Ceramic Materials," *Doklady Akademii Nauk SSSR,* Vol. 67, No. 5, May 1949, pp. 831–834.

[4] Ryshkewitch, E., "Compression Strength of Porous Sintered Alumina and Zirconia," *Journal of the American Ceramic Society,* Vol. 36, No. 2, Feb. 1953, pp. 65–68.

[5] Duckworth, W., "Discussion of Ryshkewitch Paper," *Journal of the American Ceramic Society,* Vol. 36, No. 2, Feb. 1953, p. 68.

[6] Knudsen, F. P., "Dependence of Mechanical Strength of Brittle Polycrystalline Specimens on Porosity and Grain Size," *Journal of the American Ceramic Society,* Vol. 42, No. 8, Aug. 1959, pp. 376–387.

[7] Goetzel, C. G., *Treatise on Powder Metallurgy,* Vol. II, Interscience, New York, 1950, p. 754.

[8] Brown, S. D., Biddulph, R. B., and Wilcox, P. D., "A Strength-Porosity Relation Involving Different Pore Geometry and Orientation," *Journal of the American Ceramic Society,* Vol. 47, No. 7, July 1964, pp. 320–322.

[9] Gelles, S., Nerses, V., and Siergiej, J., "Beryllium as a Structural Material," *Journal of Metals,* Vol. 15, Nov. 1963, pp. 843–848.

[10] Heck, F. W., Ferriss, D. P., Mott, L. H., and Comstock, G. J., "The Investigation of Porous Media Prepared from Spherical Metal Powder Particles," WADC TR-54-183, March 1955, Stevens Institute of Technology, Hoboken, N.J.

[11] Carman, P. C., *Flow of Gases through Porous Media,* Butterworths Scientific Publications, London, 1956, pp. 50ff.